Catadioptric null test of ultra-deep concave aspheric lens in wide-field optical system

Xing Zhong* and Guang Jin

National & Local United Engineering Research Center of Small Satellite Technology, Changchun Institute of Optics, Fine Mechanics and Physics, Chinese Academy of Sciences, Changchun, Jilin 130033, China

*Corresponding author: ciomper@163.com

Received 2 April 2013; revised 30 May 2013; accepted 5 June 2013;
posted 6 June 2013 (Doc. ID 188161); published 28 June 2013

To test the ultra-deep conic surface in wide-field optical systems, a catadioptric null test method is researched in this paper. Equations of infinite conjugate null test system are established and solved using optical path length. The numeric results of a self-aligning mirror's shapes are fitted by coefficients and validation is done in optical design software. The rms wavefront error is 0.0019λ ($\lambda = 632.8$ nm) in the example fitted by five coefficients. Furthermore, by adjusting spherical aberration distributions, an all-spherical finite conjugate null test system is designed, whose rms wavefront error is 0.0309λ. The test methods in this paper have been proven to be adaptive to many other similar ultra-deep surfaces, even with higher orders. © 2013 Optical Society of America

OCIS codes: (120.3180) Interferometry; (220.4840) Testing; (120.6650) Surface measurements, figure.

http://dx.doi.org/10.1364/AO.52.004738

1. Introduction

In optical system design, aberrations corrected by aspheric surfaces are decided by their positions. Aspheric surfaces nearby stop mainly correct high-order spherical aberration related to aperture radius, while surfaces far from stop mainly correct high-order astigmatism and distortion related to field angle. It is extremely important for wide-field optical systems that the forehead negative lenses reduce angle of incident ray and height of ray incident to consequent lens, and make aberrations corrected easier. Designers have found that the first negative lens using an aspheric surface in wide-field optical systems can not only correct aberration well, but also increase the uniformity of the image plane's illumination. These types of surfaces are usually deep concave in many designs [1,2].

Recently, thanks to the progress of optical manufacturing technology, aspheric surfaces are widely used [3]. But the deep concave aspheric surfaces' application is limited, because to manufacture them special polishing tools are needed and methods are used that make it difficult. At the same time, an important reason for the limitation is that there are not many methods to test its surface accuracy precisely. Generally, the noncontact optical test methods have more advantages on accuracy and efficiency than contact methods [4]. The null test, based on laser interferometers, is the most widely used noncontact method and is composed of compensated optical elements (lens, mirror, computer-generated hologram, etc.) and the element under test [5–7]. In a common null test, the surface under test is treated as a reflector. The obverse test is realized by the rays' self-aligning reflection on this surface, for example, the Offner compensator's test system [8]. The Offner compensator produces a divergent test beam to correct the aspheric surface's aberration with normal incident rays reflecting on the surface. But for an ultra-deep aspheric surface, this cannot be accomplished because the solid angle of the test beam is beyond 2π and can hardly be produced. Therefore,

1559-128X/13/194738-05$15.00/0

in this paper, we tried to find a new null test method to avoid this problem. We take the ultra-deep concave aspheric lens as a refractive element, and the null test is realized with aberrations corrected by an auxiliary mirror. The design result shows this might be a very promising way to solve the test problem for an ultra-deep aspheric lens.

2. Typical Ultra-Deep Concave Aspheric Lens

A typical ultra-deep concave aspheric surface used in a wide-field optical system's first negative lens is shown in Fig. 1. This is a 100 mm focal length aerial photograph optical system whose diagonal angle of view is 94° and relative aperture is 1/5.6. Its average modulate transfer function (MTF) at 50 lp/mm is above 0.6, relative illumination of marginal field is above 50%. The performance of its MTF and relative illumination is hard to achieve by all-spherical designs.

The first lens's concave aspheric surface of the optical system shown in Fig. 1 is described by [9]:

$$Z(r) = \frac{cr^2}{1 + \sqrt{1 - (1+K)c^2r^2}}, \tag{1}$$

where c is the curvature, K is the conic constant ($c = 0.01282$, $K = -0.56766$ in our case), and r is the radial coordinate in lens units. The diameter of the aspheric surface is 195 mm while its radius is 78 mm, so its relative aperture achieves 1/0.2. Test problems of the ultra-deep concave surface must be solved first to realize its highly accurate polishing.

3. Infinite Conjugate Null Test with a Mirror

A. Principle

The first negative lens of the wide-field optical system reduces the angle between chief rays of the paraxial field and oblique field. To reduce the diameter of the test beam, taking advantage of the lens' ray deflecting character, inversed ray tracing is done with parallel incident rays into the concave surface. An orthogonal coordinate is established to model the ray tracing, as shown in Fig. 2. Point O is the vertex of the aspheric surface under test, and $P(x_0, y_0)$ is the intersection of the parallel incident rays and the

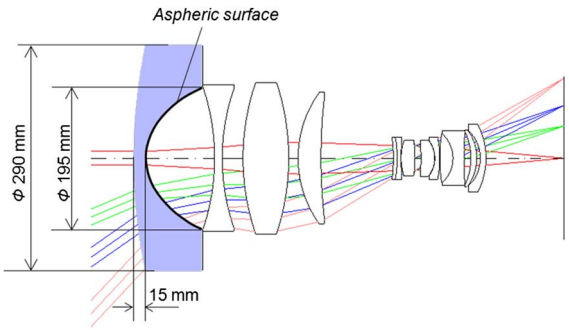

Fig. 1. Ultra-deep concave aspheric surface used in a wide-field optical system.

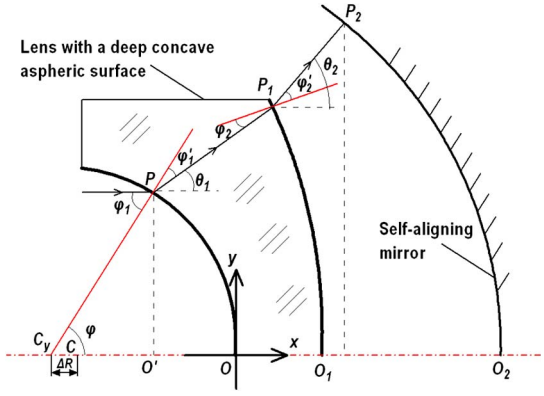

Fig. 2. Ray tracing of an ultra-deep aspheric lens.

aspheric surface. For a null test, a mirror located at O_2 is supposed to be self-aligning to incident rays.

The incident ray angle φ_1 can be solved by normal aberration character of conic surface [10]. In Fig. 2, point C_y is the intersection of the concave surface's normal and x axis, and point C is the curvature center of the surface's vertex. The distance ΔR between C_y and C is a so called normal aberration of conic surface. By definition in analytic geometry, we can get

$$\Delta R = -kx_0, \tag{2}$$

so

$$|C_yO'| = \frac{1}{c} + \Delta R - x_0 = \frac{1 - c(1+k)x_0}{c}, \tag{3}$$

$$\tan\varphi = \frac{y_0}{|C_yO'|} = \frac{cy_0}{1 - c(1+k)x_0}, \tag{4}$$

then

$$\varphi_1 = \varphi = \arctan\left[\frac{cy_0}{1 - c(1+k)x_0}\right], \tag{5}$$

and the refracted ray angle φ_1' is solved by Snell's law:

$$\varphi_1' = \arcsin\left[\frac{\sin\varphi_1}{n}\right], \tag{6}$$

so the slope of PP_1 is

$$k_1 = \tan\theta_1 = \tan(|\varphi_1| - |\varphi_1'|). \tag{7}$$

The coordinates of intersection $P_1(x_1, y_1)$ of rays and a convex sphere can be acquired by solving the equations below:

$$\begin{cases} y - y_0 = k_1(x - x_0) \\ y^2 + (x + R - l_2)^2 = R^2 \end{cases}, \tag{8}$$

where R is the radius of convex sphere, l_2 is the central thickness of lens, $l_2 = |OO_1| = 15$ mm.

Equation (8) is solved and positive roots are acquired as

$$\begin{cases} x_1 = x_0 - \frac{y_0}{k_1} + \frac{y_0 + k_1(l_2 - R - x_0 + \sqrt{A})}{k_1(k_1^2+1)} \\ y_1 = \frac{y_0 + k_1(l_2 - R - x_0 + \sqrt{A})}{k_1^2+1} \end{cases}, \tag{9}$$

where A is defined by

$$A = R^2 + 2Rk_1(y_0 + l_2k_1 - k_1x_0) - l_2k_1(2y_0 + l_2k_1 - 2k_1x_0) - k_1x_0(k_1x_0 - 2y_0) - y_0^2.$$

The refracted angle φ_2 and φ_2' are

$$\varphi_2 = \theta_1 - \left| \arctan\left(-\frac{y_1}{\sqrt{R^2 - y_1^2}} \right) \right|, \tag{10}$$

$$\varphi_2' = \arcsin(n \cdot \sin|\varphi_2|), \tag{11}$$

so the slope of P_1P_2 is

$$k_2 = \tan\theta_2 = \tan\left[\left| \arctan\left(-\frac{y_1}{\sqrt{R^2 - y_1^2}} \right) \right| + \varphi_2' \right]. \tag{12}$$

The coordinates of point $P_2(x_2, y_2)$ on a self-aligning mirror can be solved from equations established similarly:

$$\begin{cases} x_2 = \frac{x_1 + d_2\sqrt{B}}{k_2} \\ y_2 = y_1 + d_2\sqrt{B} \end{cases}, \tag{13}$$

where $d_2 = |P_1P_2|$ and B are defined by

$$B = \frac{1}{k_2^2 + 1}.$$

Therefore, we find that if d_2 is known, the surface shape of self-aligning mirror can be calculated from any concave surface under test with its shape given.

B. d_2 Solved by Optical Path Length

For parallel incident rays, PO' is taken as the plane wavefront's reference. According to the mirror's self-aligning condition in null test, we can get the relations of an optical path length:

$$n|PP_1| + |P_1P_2| = |O'O| + n|OO_1| + |O_1O_2|, \tag{14}$$

then

$$d_2 = |P_1P_2| = |x_0| + nl_1 + |O_1O_2| - n\left| \sqrt{(x_1 - x_0)^2 + (y_1 - y_0)^2} \right|, \tag{15}$$

where $|O_1O_2|$ is the air space between the mirror and lens under test. It is fixed and can be given in a reasonable range in an actual null test. Now, we can get the surface function of a self-aligning mirror, which is described by coordinates of $P_2(x_2, y_2)$ calculated from given coordinates of $P(x_0, y_0)$.

C. Numerical Calculation and Surface Fitting

The calculated numerical results of the mirror's surface sag by different $|O_1O_2|$ are shown in Fig. 3. It is shown that, the larger the $|O_1O_2|$, the larger the diameter of the self-aligning mirror, the planer the surface shape will be.

We use an even asphere polynomial [11] with fourth-, sixth-, and eighth-order terms (the second-order term is not used to avoid the fitting error caused by its coupling with conic term) to fit the calculated numerical results, which are described by

$$Z'(r) = \frac{cr^2}{1 + \sqrt{1 - (1+K)c^2r^2}} + a_2r^4 + a_3r^6 + a_4r^8. \tag{16}$$

The fitting coefficients are shown in Table 1.

D. Validation in ZEMAX

The condition $|O_1O_2| = 100$ mm is taken for example in the validation. Using the coefficients of fitted even asphere shown in Table 1, parameters of the infinite conjugate null test system are inputted in ZEMAX optical design software, and its layout is shown in Fig. 4. The wavefront error is shown in Fig. 5, whose rms value is 0.0019λ.

It is noticeable that, if there are enough aspheric coefficients in the fitting, theoretically, the surface shapes acquired by numerical calculation will be perfect, and there will be no wavefront error. But these

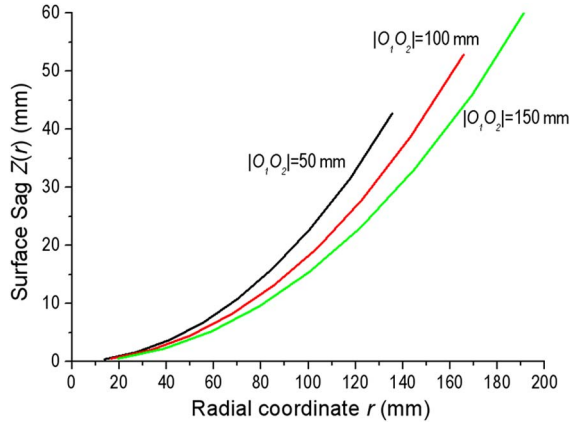

Fig. 3. Surface sag of self-aligning mirror versus a radial coordinate.

Table 1. Surface Fitting Coefficients

	$\lvert O_1O_2\rvert = 150$ mm	$\lvert O_1O_2\rvert = 100$ mm	$\lvert O_1O_2\rvert = 150$ mm
c	−4.323E − 3	−3.554E − 3	−3.018E − 3
K	−0.04150	−0.03427	−0.02894
a_2	2.479E − 9	1.133E − 9	5.894E − 10
a_3	4.317E − 15	2.114E − 15	1.008E − 15
a_4	2.203E − 19	4.111E − 20	1.031E − 20

types of surface shapes only have mathematic meaning. The extremely complex aspheric mirrors are very difficult to be manufactured themselves.

Although the catadioptric null test, compensated by single mirror in this section, needs other aspherical elements, the surface of the mirror used is much planer than the surface under test. So it can be tested in traditional ways using compensators that are easily manufactured. Volume producing of the lens will reduce cost and make it acceptable to producers (for infrared applications, the diamond turning mirror will satisfy the demand, and will not cost too much). The auxiliary mirror's cost-benefit relationship can be evaluated using the calculated results above before manufacture, and will usually depend on its diameter and the manufacturing techniques.

On the other hand, except for the disadvantage of using aspheres, the test is realized by parallel rays in this section. So, it needs the interferometer to have the same aperture as the surface under test, going against the miniaturization of the test system. Therefore, for a better application of the test method in this paper, all spherical finite conjugate null tests of ultra-deep concave aspherical surfaces are researched further.

4. All-Spherical Finite Conjugate Null Test System

The sum of all optical elements' spherical aberration in the null test is

$$S_{\mathrm{I}}^{t} + S_{\mathrm{I}}^{c} = 0, \tag{17}$$

where S_{I}^{t} is the spherical aberration contributed by surface under test, and S_{I}^{c} is the spherical aberration contributed by compensated elements.

First, the spherical aberration of the lens under test is analyzed with the parallel incident rays according to the null test system in Section 3. The lens under test is composed of a sphere and a conic

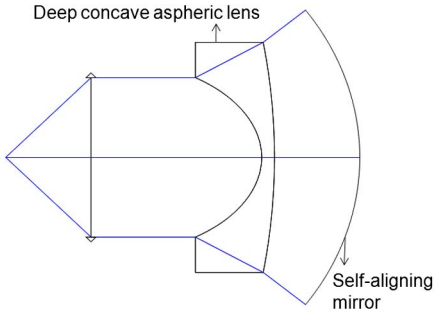

Fig. 4. Layout of infinite conjugated test system.

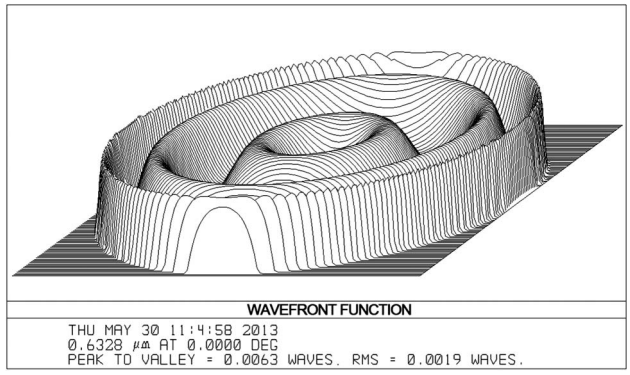

Fig. 5. Wavefront error of infinite conjugated test system.

asphere. The coefficient of primary spherical aberration of the spherical surface is

$$S_{\mathrm{I}} = -[n(u + yc)]^2 y\left(\frac{u'}{n'} - \frac{u}{n}\right), \tag{18}$$

and the coefficient of primary spherical aberration of the conic surface can be calculated as [12]

$$S_{\mathrm{I}}' = S_{\mathrm{I}} + y^4 c^3 K(n' - n), \tag{19}$$

so we can get the primary spherical aberration of lens under test with the parallel incident rays using the parameters of optical system, which is

$$S_{\mathrm{I}}^{t} = S_{\mathrm{I}} + S_{\mathrm{I}}' = 7.416.$$

The mirror in Section 3 is supposed to be spherical, so its self-aligning means aplanatic, i.e., the mirror's spherical aberration is zero. Therefore, new compensated optical elements with spherical aberration contribution $S_{\mathrm{I}}^{c} = -S_{\mathrm{I}}^{t}$ must be involved to satisfy Eq. (17).

A positive lens, L1, must at least be used to realize a finite conjugated null test. L1 refracts rays from the focus of the interferometer's standard lens so they are approximately parallel. It can be deduced that no matter what shape L1 is, its spherical aberration contribution is positive, the same as the lens under test. (A convex-plane lens is adapted as L1 in this paper.) Another lens, L2, with abundant negative spherical aberration, should be introduced. A negative meniscus shaped lens is competent for this work. The initial configuration of L2 can be calculated through ray tracing and the spherical aberration formula. By trials in optical design software, we found it can correct high-order spherical aberration better than L2 with its concave surface facing the surface under test. The final all-spherical design is shown in Fig. 6, and the wavefront error is shown in Fig. 7. Its rms value is 0.0309λ.

Because the deep concave lens in the wide-field optical system is always assembled far from stop, incident rays of any field occupy a small area on the lens' surface. Contribution of its surface error to system's

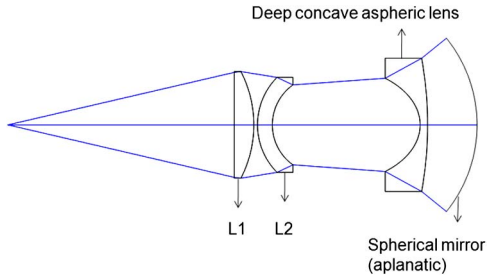

Fig. 6. Layout of the all-spherical finite conjugate null test system.

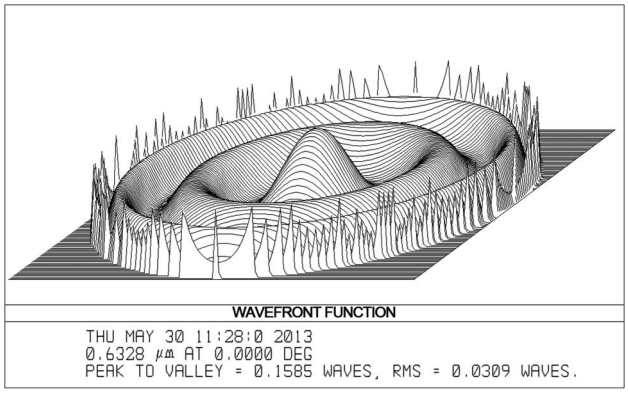

Fig. 7. Wave-front-error of all-spherical finite conjugate null test system.

wavefront is much less than a lens close to stop. Based on data above, the influence of all-spherical design's wavefront-error is evaluated, and the results show that the lens' test requirement of wide-field optical systems for imaging aims can be matched.

The alignment of this all-spherical test system is similar to other null test systems. The two compensated lenses can be mounted in a barrel and aligned by the precise centering method. The alignment of the system can be realized by a computer aided aligning method using wavefront data provided by interferometers.

5. Conclusions

The null test method of ultra-deep concave aspherical surface in wide-field optical systems is researched in this paper and design results are given. The disadvantages of a usual obverse test can be avoided by a whole test of the lens in a catadioptric system using a mirror. When being manufactured, the convex sphere of this kind of lens can be finished beforehand, and the concave surface can be manufactured first with the help of contact test methods. To highly increase the surface accuracy, the method in this paper will be helpful in the polishing process. It has been proven that the method in this paper has a good adaptability to different types of aspherical surfaces (elliptical surfaces, hyperboloidal surfaces, high-order aspherical surfaces, etc.), and this method can be applied in many other similar ultra-deep concave surface tests.

References

1. N. A. Agal'tsova, *Atlas of Aerial photographic lenses "Russar"* (Science, 2010).
2. W. Yongzhong, *Fish-eye Lens Optics* (Science, 2006).
3. S. Bambrick, M. Bechtold, and S. DeFisher, "Recent developments in finishing of deep concave, aspheric, and plano surfaces utilizing the ultraform 5-axes computer controlled system," Proc. SPIE **7302**, 73020U (2009).
4. D. Malacara, *Optical Shop Testing* (China Machine, 1983).
5. T. Kim and J. H. Burge, "Null test for a highly paraboloidal mirror," Appl. Opt. **43**, 3614–3618 (2004).
6. R. Pursel, "Null testing of a f/0.6 concave aspheric surface," Proc. SPIE **2263**, 210–217 (1994).
7. J. Burge, "A null test for null correctors: error analysis," Proc. SPIE **1993**, 86–97 (1993).
8. A. Offner, "A null corrector for paraboloidal mirrors," Appl. Opt. **2**, 153–155 (1963).
9. L. Jones, "Reflective and catadioptric objectives," in *Handbook of Optics*, M. Bass, ed. (McGraw-Hill, 1995), **II** p. 18.3.
10. P. Jun-hua, *Design, Machining and Testing of Optical Aspheric Surface* (Science, 1994).
11. ZEMAX Optical Design Program User's Guide (ZEMAX, 2009).
12. R. Kingslake, *Lens Design Fundamentals*, 2nd ed. (Academic, 2010).